Arctic Vortex changes alter the sources and isotopic values of precipitation in northeastern US

Tamir Puntsag[1*], Myron J Mitchell[1], John L Campbell[2], Eric S Klein[3], Gene E Likens[4] and Jeffrey M Welker[3]

[1]SUNY-ESF, Syracuse, NY 13210, USA

[2] US Forest Service, Northern Research Station, Durham, NH 03824, USA

[3]University of Alaska Anchorage, Biological Sciences Department, AK 99508, USA

[4]Cary Institute of Ecosystem Studies, Millbrook, NY 12545, USA and University of Connecticut, Department of Ecology and Evolutionary Biology, Storrs, CT 06269, USA

*tpuntsag@syr.edu

Abstract

Altered atmospheric circulation, reductions in Arctic sea ice, ocean warming, and changes in evaporation and transpiration are driving changes in the global hydrologic cycle. Precipitation isotopic ($\delta^{18}O$ and $\delta^{2}H$) measurements can help provide a mechanistic understanding of hydrologic change at global and regional scales. To study the changing water cycle in the northeastern US, we examined the longest (1968-2010) record of precipitation isotope values, collected at the Hubbard Brook Experimental Forest in New Hampshire, US (43°56'N, 71°45'W). We found a significant reduction in $\delta^{18}O$ and $\delta^{2}H$ values over the 43-year record, coupled with a significant increase in *d-excess* values. This gradual reduction in $\delta^{18}O$ and $\delta^{2}H$ values unexpectedly occurred during a period of regional warming. We provide evidence that these changes are governed by the interactions among the Atlantic Multidecadal Oscillation, loss

of Arctic sea ice, the fluctuating jet stream, and regular incursions of polar air into the northeastern US.

Introduction

The global water cycle is exhibiting dramatic changes as surface air and sea surface temperatures have increased, perennial sea-ice has decreased, droughts have become more extreme, severe flooding due to sea level rise and protracted winter storms have become more common, and precipitation variability has increased (e.g., heavy downpours are likely to occur more frequently in the Northeast) [1,2]. For example, in the winter of 2013-2014 there was a prolonged meridional flow across North America that led to an abnormally cold and snowy winter in the eastern US, a prolonged drought in the western US, and unusually warm winter temperatures across Alaska[2]. The mechanisms controlling these changes are complex and include altered atmospheric circulation, reductions in Arctic sea ice, ocean warming, and changes in evaporation on water bodies (lakes, seas and oceans) and transpiration[3]. Because isotope ($\delta^{18}O$ and $\delta^{2}H$values) ratios in precipitation have been shown to respond to climate oscillations and other abiotic influences, they provide a powerful tool to help understand the underlying processes affecting hydrologic changes at global and regional scales[4–8].

Condensation and evaporation influence water isotopic ($\delta^{18}O$ and $\delta^{2}H$) values at both global[9] and continental-scales, creating predictable patterns of precipitation geochemistry[4,10,11]. These water isotopic fractionation processes are influenced by various physical factors, including temperature[12,13]. However, it has been shown that other critical factors including moisture sources[14], air mass trajectory[5], seasonality[14], and teleconnections [e.g., Pacific North American (PNA) and El Niño Southern Oscillation (ENSO)], collectively influence the water cycle and

47 isotopologues of preciptation[8,12]. Climatic influences and storm track effects on precipitation
48 isotopes have been primarily examined for western North America[4,5,11] or over short-time
49 periods in the eastern US[14]. A long-term perspective is needed, however, to evaluate fluctuations
50 in climate phases and shifts in storm track patterns. We expect that climate change indices,
51 including the Atlantic Multidecadal Oscillation (AMO), the North Atlantic Oscillation (NAO),
52 and the Arctic Oscillation (AO), may show linkages to changes in precipitation isotopes[15]. In our
53 study we show that *d-excess* ($\delta^2H-8\times\delta^{18}O$) values provide new information on water sources
54 affected by evaporation or other non-equilibrium phase changes such as diffusion and
55 dissociation reactions[10].

56 To examine long-term trends in the hydrologic cycle of the northeastern US, we developed
57 the longest (1968-2010)[4,8,12,16] continuous record of precipitation isotopes available, using
58 archived samples collected at the Hubbard Brook Experimental Forest (HBEF). A substantial
59 amount of past research incorporates natural paleoclimatic records (e.g., ice cores, lake
60 sediments, tree rings, limestone caves, and groundwater) that preserve the isotopic composition
61 of water and are useful in evaluating the relationships between climatic variables and
62 precipitation $\delta^{18}O$ values. However, relatively little research has investigated modern
63 relationships between stable isotopologues of water and climatic patterns over extended periods
64 (i.e., decades). Our study provides new information on the modern record of precipitation and
65 how isotopic values ($\delta^{18}O$ and δ^2H) and *d-excess* reflect the sources of precipitation and how
66 they have changed in response to climatic changes over the past 43 years.

67

68 **Results**

69 **Long-term trends**. We found significant positive trends in mean annual *d-excess* values
70 ($P<0.0001$) and surface air temperatures ($P=0.005$), whereas $\delta^{18}O$ ($P<0.0001$) and $\delta^{2}H$
71 ($P=0.0003$) values showed significant declines over the 43-year period (Fig.1a-e). Average
72 annual surface air temperatures ranged from a minimum of 3.2^{o}C in 1980 to a maximum of 6.1^{o}C
73 in 1998 over the 43 years (Fig.1a.). The precipitation amounts ranged from a minimum of 100
74 cm in 2001 to a maximum of 180 cm in 1973 (Fig.1b). Annual isotopic values weighted by
75 monthly precipitation amounts for $\delta^{18}O$ ranged from a relatively high value of -6.5‰ in 1973
76 (the wettest year[16]) to a low value of -12‰ in 1997 (Fig.1c) while $\delta^{2}H$ values for these same
77 years were -46‰ and -80‰ respectively (Fig.1d). Annual *d-excess* values ranged from a low
78 value of 0.2‰ in 1978 to a high value of 22‰ in 2008 (Fig.1e). Based on the significant linear
79 relationship ($P=0.02$), a 1^{o}C change in temperature resulted in a -0.61‰ change in the $\delta^{18}O$
80 values from 1968-2010, whereas the *d-excess* and surface air temperature values were positively
81 related ($P<0.0001$) with a slope of 4.6‰ /1^{o}C. Over the 43-year record, the annual average *d-*
82 *excess* values increased from ~ 4‰ to 21‰, weighted annual $\delta^{18}O$ values declined from -8.9‰
83 to -11.5‰, and $\delta^{2}H$ values declined from -66.7‰ to -70.3‰ (Fig.1c, d, e).
84 The progressive reduction in $\delta^{18}O$ and $\delta^{2}H$ values during our study period differs from some
85 global and regional results, which have shown that $\delta^{18}O$ and $\delta^{2}H$ values of precipitation increase
86 with mean annual surface air temperatures[9,10]. However, temperature generally only accounts for
87 approximately 50-60% of the variance[4,9,13] in precipitation isotopic values, indicating that other
88 processes, such as climate oscillations, moisture sources and changes in atmospheric circulation
89 are also important controlling mechanisms[4–6,8,17]. To further explore the influence of climate
90 change on the isotopic composition of precipitation, we examined the correspondence between
91 climate oscillations and the $\delta^{18}O$ and *d-excess* values for precipitation at the HBEF over the last

four decades, including the AMO[18–21], AO[22], NAO[23], and PNA[5]. The AMO is a North Atlantic Ocean current (0-70^{o}N) with decadal modes that affect sea surface temperature variability; the AO and NAO reflect sea level pressure anomalies poleward of 20^{o}N and opposing variations of barometric pressure near Iceland and the Azores; the PNA reflects an atmospheric large-scale wave pattern featuring a sequence of tropospheric high and low pressure anomalies stretching from the subtropical west pacific to the east coast of North America. We found that only the AMO was significantly ($P<0.0001$) related to HBEF precipitation $\delta^{18}O$, $\delta^{2}H$ and *d-excess* values (Supplementary Table S1 and Fig. S2). A multi-decadal fluctuation in the North Atlantic, in which sea surface temperature exhibited a positive phase from 1968 to 1994 and a negative phase from 1995 to 2010 with a temperature range of ~0.4^{o}C (Fig.2a). All oscillations were associated with variation in the direction and strength of the prevailing circulation and storm track affecting moisture sources, temperature and precipitation amounts that were most strongly expressed in winter, but affected climate throughout the year.

Influential factors on precipitation isotopes. We performed stepwise multiple-regression (mixed option) for both $\delta^{18}O$ and *d-excess* values as dependent variables, and mean annual temperature (°C), precipitation amount (mm), AMO, NAO, PNA, and AO indices as independent variables as a means of resolving the multitude of potential factors influencing our isotopic values in precipitation. We found that 84% of the variation in *d-excess* (adjusted $r^2=0.84$; RMSE=2.5) was explained by AMO, precipitation amount, and AO, as described by the following equation (1) (Fig.S3b).

$$d\text{-}excess = 7.60 + (34.92 \times AMO) + (0.0035 \times Precip) + (1.297 \times AO) \quad (1)$$

For $\delta^{18}O$ values, AMO index and mean annual temperature explained 70% of the variation of $\delta^{18}O$ values (adjusted r^2=0.70; RMSE=0.74) as described by the following equation (2) (Fig.S3a).

$$\delta^{18}O = -11.19 + (-7.561 \times AMO) + (0.2801 \times Temp) \quad (2)$$

These analyses support our hypothesis that the AMO played a dominant role in affecting HBEF precipitation *d-excess* values, with the AO and local precipitation amounts having a significant, but secondary effect based on the smaller, t-test P values (below α_e=0.15) in the stepwise model. Similarly for the $\delta^{18}O$ values, the AMO values also had the strongest influence, with local mean annual temperature values having a secondary, but significantly important contribution to the variance in $\delta^{18}O$ values. The AMO index does not reflect a specific climate pattern (jet stream flow trait), but rather reflects ocean warming and any secondary consequences of that warming at large spatial scales[18,24]. During our study period, there was an increasing trend in AMO values (as measured by the AMO anomaly based on decadal changes in sea surface temperature) from -0.25 to +0.35, which corresponded with a positive trend in *d-excess* values from ~0 to 22‰ and decrease in the $\delta^{18}O$ values from ~-7 to -12‰ (Fig.2a).

The progressive increase in *d-excess* values indicates that precipitation moisture sources during our study (1968-2010) were increasingly from colder northern regions; an observation similar to a much shorter-term study on the role of Arctic moisture sources on the precipitation isotope geochemistry in the northeastern US[14,25]. This previous study[14] used back trajectories of daily precipitation isotope values between 1999-2001 to show that this region receives moisture from the Arctic ~15% of the time, with *d-excess* values of ~19‰, and that this moisture source typically occurs during the fall and winter. Thus, increases in the frequency of Arctic moisture sources have the potential to influence the average annual isotopic values of sites in the

137 northeastern US. When surface air temperatures in these northern regions are near the freezing
138 point of water, the ratios of the ice/vapor fractionation factor are higher for δ^2H compared to
139 $\delta^{18}O$ due to the greater fractionation of hydrogen isotopes under these conditions[17,26]. Hence,
140 greater *d-excess* values may reflect moisture sources that are derived from colder and drier
141 climates compared to moisture sources associated with more humid and warmer climates[17,26,27].
142 Also, during positive AMO conditions, the North Atlantic jet stream and storm tracks shift
143 southward, leading to incursions of air from higher latitudes across the eastern US and northern
144 Europe[24,28]. Often *d-excess* changes are indicative of shifts in moisture sources, with low *d-*
145 *excess* values associated with substantial evaporation in coastal zones, and high values associated
146 with moisture sources over terrestrial regions characterized by substantial amounts of water
147 recycled from plant transpiration[29].

148

149 **Discussion**

150 **Mechanisms controlling precipitation isotope trends.** Complex changes in climate and
151 synoptic weather patterns, with various climatic controls predicted by numeric models[24,30], are
152 the apparent mechanisms controlling the long-term changes in isotopic values of northeastern US
153 precipitation. Arctic amplifications (1990-2010) and North Atlantic regional air temperature
154 increases corresponded to a concomitant warming of the North Atlantic Ocean (0.031^{o}C per
155 decade during the period of 1900-1999[23] and ~0.4^{o}C per decade from 1990-2008[19,20]).
156 Additionally, sea ice extent in the Arctic has decreased in concert with a general weakening of
157 the polar vortex, leading to weakened west-to-east winds, and ultimately a more north/south
158 meandering in the jet steam, allowing cold air excursions to become more frequent in the eastern
159 US[19,24,31]. The markedly warmer Arctic, with decreased cover of sea ice in fall and early winter,

160 has led to larger heat fluxes from the ocean to the polar stratosphere and a weakening of Arctic
161 vortex and negative AO values, especially in mid-winter (January-February)[32]. This weakened
162 polar vortex has resulted in changing weather patterns, especially at mid-latitudes. We propose
163 that these changes in synoptic weather patterns (storm tracks) have resulted in the delivery of
164 more frequent precipitation events from the north, which has led to a decline in $\delta^{18}O$ and $\delta^{2}H$
165 values and an increase in *d-excess* values for precipitation at the HBEF during a period of
166 regional warming. These results are in contrast to most previous interpretations of declining
167 isotopic values of precipitation associated with climate, which suggested that the declining
168 values are a function of cooling atmospheric temperatures without incorporating the influence of
169 moisture source changes[12]. These trends in $\delta^{18}O$, $\delta^{2}H$ and *d-excess* values were also apparent
170 during a shorter sampling period (1989-2003) at a site in northern Vermont[8].
171 Fall sea ice in the Arctic Ocean has declined at a rate of 12.4%/decade since 1979, leading to
172 progressively larger Arctic Ocean heat fluxes that impact the jet stream in a weaker zonal jet
173 with larger meanders and more persistent extreme weather[24,31]. During this same period, $\delta^{2}H$
174 and $\delta^{18}O$ values at the HBEF have declined, while *d-excess* values have increased (Fig.2b),
175 suggesting a shift to an increased proportion of northern moisture sources. If these changes in the
176 jet stream, which allow more air from the Arctic to cascade south into the northeastern US, were
177 associated with a decrease in fall Arctic Ocean sea ice extent, it would be expected that the
178 greatest isotopic changes in precipitation should occur in the fall and winter. This seasonal
179 expectation is consistent with our findings at the HBEF, as most of the long-term annual changes
180 in precipitation isotopic values were in the fall and winter periods (Fig.2b). Corroborating
181 evidence for a seasonal, as well as a moisture source shift is provided by marine aerosol
182 studies[33]. For instance, from 1967 to 1994, trends in $\delta^{34}S$ values in precipitation were positively

183 correlated with marine SO_4^{2-} concentrations; winter (6%) marine contributions were higher than
184 summer (3%) contributions[33]. Also, Ottawa in Ontario, Canada (45°32'N, 75°60'W) which is
185 farther to the west and an inland site also shows a generally increasing trend in the average
186 annual $\delta^{18}O$ values of precipitation, but the trend was not statistically significant for 1970-
187 2007[34] . The Ottawa site mean temperature was (6.1°C) and was about 1.7°C warmer than the
188 HBEF site (4.4°C) during this study; however this research showed a similar positive relationship
189 between monthly $\delta^{18}O$ in precipitation and temperature. It should be noted that at both sites the
190 seasonal temperature ranges were much greater than long -term temperature ranges, making it
191 challenging to evaluate the effects of long-term changes in temperature on precipitation isotopic
192 values. Therefore, we suggest that the two studies are consistent with respect to seasonal
193 temperature effects with the summer having the highest $\delta^{18}O$ values and the winter the
194 lowest. These observations further support our interpretation of how interrelated changes in
195 synoptic climatology are driving long-term trends $\delta^{18}O$, $\delta^{2}H$ and *d-excess* values in northeastern
196 precipitation.

197 The large changes in precipitation isotopes during the fall further suggest that the AMO
198 captures important factors that lead to changes in large, spatial scale weather and moisture
199 sources, including the generation of storms in the northeastern US derived from relatively cold
200 and dry moisture sources (i.e., the Arctic). Air parcel back trajectories demonstrate how colder
201 northern-sourced moisture can influence the isotopic patterns apparent in the long-term record
202 (Fig 3a-e). In November 2014 a polar vortex[35] extended into the eastern US during a positive
203 phase of the AMO. The result of this event, which ended ~November 18, was mixed rain-snow
204 with comparatively low $\delta^{18}O$ (-16‰) and high *d-excess* values (20‰). We also did isotopic
205 analyses on precipitation events before the November event (Fig.3f). A progressive increase in

206 the frequency of these largely seasonal incursions of colder northern air would result in the
207 isotope patterns we observed in the long-term isotope record at the HBEF.

208 Additionally, temporal variations of air parcel back trajectories were estimated for the highest
209 precipitation amounts for a day in November (last full month of fall) from 1968 to 2010 and
210 compared with *d-excess* and $\delta^{18}O$ values of precipitation (Fig.4). These back-trajectory analyses
211 were used for temporally constraining the spatial precipitation sources. We used the day with the
212 highest daily precipitation as well as the day before and after the highest daily precipitation day
213 for the November of each year. Precipitation amounts derived from these three daily air masses
214 (72- h period) ranged from 24 to73% of the total November precipitation for our study period.
215 This analysis indicates that the vast majority (11 of 16) of high *d-excess* values in
216 precipitation were derived from northern sources, including the Arctic and North Atlantic, during
217 the positive phase of AMO (Fig.4). The highest (2007) and the lowest (1972) *d-excess* values of
218 precipitation were, however, both associated with moisture sources from the Arctic. The isotopic
219 and trajectory data suggest that the moisture sources during these two events in 2007 and 1972
220 were from: a) a humid (open Hudson Bay) region, with relatively high $\delta^{18}O$ and low *d-excess*
221 values and b) an arid region, with relatively low $\delta^{18}O$ and high *d-excess* values of precipitation
222 (Fig.4). Conversely, continental sources tended to dominate during negative AMO phases.

223 We have established that $\delta^{18}O$ and $\delta^{2}H$ values in precipitation decreased while *d-excess*
224 values increased over a 43-year period in the northeastern US and that these changes were linked
225 with the Atlantic Ocean-Arctic amplification interactions. A broad conceptual overview of our
226 results is provided in Fig. 5. A growing body of evidence suggests that the extreme cold that has
227 occurred in the northeastern US in the fall and winter is a pattern we can expect to continue with
228 increasing frequency as climate change progresses. This climatic pattern is due in part to Arctic

229 warming which has been twice as rapid as that in the mid-latitudes. One result of this climatic
230 shift is that the temperature differences between the Arctic and mid-latitudes are shrinking.
231 These temperature patterns affect the polar vortex which is a sinistral swirling mass of cold air
232 that spreads over the Arctic. The weakening of the Arctic and mid-latitude temperature
233 differences leads to greater undulations of the polar vortex that causes larger excursions of cold
234 air southward into the mid-latitudes, including the northeastern US. The isotopic trends found in
235 our study will likely continue and possibly become stronger with the expected further weakening
236 of the polar vortex [21, 24,32]. In addition to understanding the factors that affect the modern isotopic
237 values of precipitation, our results have important implications for the interpretation of hydrogen
238 and oxygen isotopes in climate proxies[36]. For instance, interpretation of tree ring records of
239 climate recorded in the ^{18}O values of cellulose can now be considered in the context of moisture
240 source shifts in the AMO, which is known to reflect multidecadal precipitation isotopic
241 anomalies, and appears to modulate hurricane and drought frequency[18].

242 Our results highlight the need to understand the influence of moisture sources and storm
243 tracks, climate phases, sea ice, and land surface traits on isotopic values in regional precipitation
244 and overall climatic patterns[4–6]. Additionally, our findings suggest that the isotope geochemistry
245 of precipitation at the HBEF and northeastern US in general reflect increased North Atlantic sea
246 surface temperatures and can be attributed in large part to increases in the proportion of Arctic
247 precipitation sources associated with the decreasing extent of sea ice[37]. Hence the use of
248 precipitation isotopes provides an additional tool for understanding changes in the northern
249 regions including warmer temperatures and increased precipitation in the northeastern US. Such
250 information should be incorporated into predictive models of regional and global climates.
251 Evaluating these patterns is critical for understanding the complexities of global climate change

and how the connections between marine and terrestrial systems influence the changing hydrologic cycle.

Methods

Site description. The Hubbard Brook Experimental Forest (HBEF) is located within the White Mountain National Forest of north central New Hampshire (43°56'N, 71°45'W), approximately 120 km northwest of the North Atlantic Ocean. The climate of the HBEF is humid continental with short, cool summers and long, cold winters[16,33]. During the fall and winter, as the colder polar air moves south, cyclonic disturbances periodically move up the east coast of the US providing an occasional source of maritime air[14,16]. The mean annual air temperature (measured between 1968 and 2010) was 4.8°C, with a monthly mean maximum of 17.5 °C in July and a monthly mean minimum of -9.6 °C in January using data collected at the base of the biogeochemical reference watershed (W6). During our study the mean annual precipitation amount was 138 cm, with a monthly maximum of 12.8 cm in August and a monthly minimum of 8.7 cm in February. On average, precipitation at the HBEF is distributed equally throughout the year with approximately 30% falling as snow. A snowpack usually covers the ground from late December until mid-April; the average annual maximum depth of 72 cm (19 cm snow water equivalent) occurs in March[38].

Sample collection and handling. Precipitation samples at Rain Gauge 11 (RG11) near the base of W6 were collected weekly in a bulk-precipitation collector consisting of a 28-cm diameter polyethylene funnel attached to Tygon® tubing leading to a 2-liter reservoir. The Tygon® tubing was looped to create a vapor barrier that minimizes evaporation. Snow for chemical

274 analysis was collected in plastic bags during the winter[16]. After chemical analysis of the major
275 solutes, the remaining samples were stored in screw-top, sealed Nalgene® bottles in the archive
276 building, where temperatures are kept between 5 and 10^{o}C. For the current study, we used
277 archived precipitation samples collected weekly from 1968, when samples were first archived,
278 through 2010 (43 years total). After compositing the weekly samples by volume (to the nearest
279 0.1 ml) into a monthly sample, the samples were shipped to the Stable Isotope Laboratory at the
280 University of Alaska in Anchorage. Event samples were collected between November 11 and 18,
281 2014, during a shift in the polar vortex. Isotopic analysis was performed using a Picarro Cavity
282 Ring Down Spectrometer (Li-1115) fitted with an auto-sampler. Each sample was analyzed six
283 times and reanalysis of the sample was done when the standard deviation of the six replicates
284 was > 0.3‰ for $\delta^{18}O$ and 3‰ for $\delta^{2}H$, or when the internal standard for the run differed from the
285 accepted value by > ±0.2‰ and 2‰ for $\delta^{18}O$ and $\delta^{2}H$, respectively. Internal standards (USGS 45
286 and 46) and processed Anchorage tap water (with a known value) were used with each tray (50
287 samples) to account for any daily drift. All results are reported relative to Vienna Standard Mean
288 Ocean Water (VSMOW) and were calibrated using IAEA VSMOW, Standard Light Antarctic
289 Precipitation (SLAP), and Greenland Ice Sheet Precipitation (GISP) standards.
290 **Data and analysis.** HBEF daily climate data (available at http:/hubbardbrook.org) from 1968 to
291 2010 were combined into monthly and annual averages. We used the NAO, PNA, AMO and AO
292 indexes from the National Oceanic and Atmospheric Administration (NOAA) and National
293 Climatic Data Center (Fig.S1). We calculated annual average temperatures and used ANOVA to
294 evaluate differences by year. We used Kendall's tau in SAS 9.1.3 for trend analysis of the
295 monthly samples to evaluate how water isotope values and surface air temperature and
296 precipitation values changed over time. Selections of climate variables were made using a

297 multiple stepwise regression approach in JMP in 5.1.1software. For all $\delta^{18}O$ and $\delta^{2}H$ values at
298 the HBEF we used weighted monthly precipitation to derive annual values ($\delta_{\text{weighted annual}}$)
299 calculated as[9]:

300 $$\boldsymbol{\delta_{Annual}} = \sum_{Dec}^{Jan} \boldsymbol{\delta_{Each\ Month}} \times \frac{\boldsymbol{Precip_{Each\ Month}}}{\boldsymbol{Precip_{Annual\ Total}}} \quad (3)$$

301 Using the NOAA's Air Resources Laboratory (ARL) HYbrid Single-Particle Lagrangian
302 Integrated Trajectory (HYSPLIT) model[39], we calculated 72-h back trajectories for air masses at
303 500 m above ground level. The 500- m back trajectories show a more easterly component
304 representing surface air drawn into an approaching frontal system. We used the National Center
305 for Atmospheric research (NCAR) Reanalysis Project data set archived by ARL for
306 meteorological data. The back trajectory end point is RG11 at the HBEF (43.950227N and -
307 71.734612W). Back trajectories and precipitation source regions were evaluated for each year at
308 our study site[14].

309 **Sample integrity for water isotope analyses.** The first objective of these determinations was to
310 evaluate the potential influence of evaporation on water isotopic values of samples stored in the
311 archives. A concern regarding the use of the archived samples for isotopic analyses is
312 evaporation/condensation and vapor exchange with external air. The local Meteoric Water Line
313 (MWL) values for the samples collected in our study were very close to that of the Global MWL
314 as well as for a site in Ottawa, Canada (Fig.S4). Only 8% of the 516 samples had *d-excess* values
315 that were less than 0‰, suggesting that our samples did not undergo significant secondary
316 evaporation during storage, preserving their integrity and isotopic reliability[8,9,26,29]. We also
317 compared our results with samples collected at similar times (i.e., within a few days) from 2006
318 to 2010 of bulk precipitation (Watershed3-RG4) near the location used in our long-term

analyses. Mineral oil was added to the RG4 collectors to prevent evaporation in the field, and samples were stored in 20 mL glass vials that were completely filled with sample water and sealed with caps that contained plastic conical inserts to remove headspace and prevent evaporation. The isotopic values for the RG4 samples (n=42) showed no substantial differences (<5% and -2‰ ($\delta^{18}O$), -8‰ ($\delta^{2}H$) heavier and 8‰ (*d-excess*) smaller) between measurements to those values from RG11 samples in the HBEF archive taken for the same month.

References

1. Karl, T. R. & Trenberth, K. E. Modern Global Climate Change. *Science* **302,** 1719–1723 (2003).

2. Peterson, D. L. in *Climate Change and United States Forests*, Vol.57 (eds. Peterson, D. Vose, J. Weynand, T*).*Ch.6, 113–148 (Springer Netherlands, 2014)

3. Jasechko, S. *et al.* Terrestrial water fluxes dominated by transpiration. *Nature* **496,** 347–350 (2013).

4. Welker, J. M. ENSO effects on δ18O, δ2H and d-excess values in precipitation across the U.S. using a high-density, long-term network (USNIP). *Rapid Commun. Mass Spectrom.* **26,** 1893–1898 (2012).

5. Liu, Z., Yoshmura, K., Bowen, G. J. & Welker, J. M. Pacific–North American Teleconnection Controls on Precipitation Isotopes (δ18O) across the Contiguous United States and Adjacent Regions: A GCM-Based Analysis. *J. Clim.* **27,** 1046–1061 (2013).

6. Winnick, M. J., Chamberlain, C. P., Caves, J. K. & Welker, J. M. Quantifying the isotopic 'continental effect'. *Earth Planet. Sci. Lett.* **406,** 123–133 (2014).

7. Liu, Z. *et al.* Paired oxygen isotope records reveal modern North American atmospheric dynamics during the Holocene. *Nat. Commun.* **5,** 3701 (2014).

8. Welker, J. M. Isotopic (δ18O) characteristics of weekly precipitation collected across the USA: an initial analysis with application to water source studies. *Hydrol. Process.* **14,** 1449–1464 (2000).

9. Rozanski, K., Araguás-Araguás, L. & Gonfiantini, R. Relation between long-term trends of oxygen-18 isotope composition of precipitation and climate. *Science* **258,** 981–985 (1992).

10. Dansgaard, W. Stable isotopes in precipitation. *Tellus A* **16,** 436–468 (1964).

11. Birks, S. J. & Edwards, T. W. D. Atmospheric circulation controls on precipitation isotope–climate relations in western Canada. *Tellus B* **61,** 566–576 (2009).

12. Rozanski, K.in *Climate Change in Continental Isotopic Records* (eds. Swart, P. Lohmann, K. Mckenzie, J. Savin, S). Ch.1, 1–36 (American Geophysical Union, 1993)

13. Vachon, R. W., Welker, J. M., White, J. W. C. & Vaughn, B. H. Moisture source temperatures and precipitation δ18O-temperature relationships across the United States. *Water Resour. Res.* **46,** W07523 (2010).

14. Sjostrom, D. J. & Welker, J. M. The influence of air mass source on the seasonal isotopic composition of precipitation, eastern USA. *J. Geochem. Explor.* **102,** 103–112 (2009).

15. Welker, J. M., Rayback, S. & Henry, G. H. R. Arctic and North Atlantic Oscillation phase changes are recorded in the isotopes ($\delta^{18}O$ and $\delta^{13}C$) of Cassiope tetragona plants. *Glob. Change Biol.* **11,** 997–1002 (2005).

16. Likens, G. E. *Biogeochemistry of a Forested Ecosystem*. (Springer Science & Business Media, 2013).

17. Jouzel, J. & Merlivat, L. Deuterium and oxygen 18 in precipitation: Modeling of the isotopic effects during snow formation. *J. Geophys. Res. Atmospheres* **89,** 11749–11757 (1984).

18. Gray, S. T., Graumlich, L. J., Betancourt, J. L. & Pederson, G. T. A tree-ring based reconstruction of the Atlantic Multidecadal Oscillation since 1567 A.D. *Geophys. Res. Lett.* **31,** L12205 (2004).

19. Knight, J. R., Folland, C. K. & Scaife, A. A. Climate impacts of the Atlantic Multidecadal Oscillation. *Geophys. Res. Lett.* **33,** L17706 (2006).

20. Hand, R., Keenlyside, N., Omrani, N.-E. & Latif, M. Simulated response to inter-annual SST variations in the Gulf Stream region. *Clim. Dyn.* **42,** 715–731 (2013).

21. Chylek, P., Folland, C. K., Lesins, G., Dubey, M. K. & Wang, M. Arctic air temperature change amplification and the Atlantic Multidecadal Oscillation. *Geophys. Res. Lett.* **36,** L14801 (2009).

22. Deser, C. On the teleconnectivity of the'Arctic Oscillation'. *Geophys. Res. Lett.* **27,** 779–782 (2000).

23. McNeil, N. & Chooprateep, S. Modeling sea surface temperatures of the North Atlantic Ocean. *Theor. Appl. Climatol.* **116,** 11–17 (2013).

24. Cohen, J. *et al.* Recent Arctic amplification and extreme mid-latitude weather. *Nat. Geosci.* **7,** 627–637 (2014).

25. Klein, E. S. *et al.* Arctic cyclone water vapor isotopes support past sea ice retreat recorded in Greenland ice. *Sci. Rep.* **5,** 10295; DOI: 10.1038/srep10295 (2015).

26. Gat, J. R. Oxygen and hydrogen isotopes in the hydrologic cycle. *Annu. Rev. Earth Planet. Sci.* **24,** 225–262 (1996).

27. Benetti, M. *et al.* Deuterium excess in marine water vapor: Dependency on relative humidity and surface wind speed during evaporation. *J. Geophys. Res. Atmospheres* **119,** 2013JD020535 (2014).

28. Francis, J. A. & Vavrus, S. J. Evidence linking Arctic amplification to extreme weather in mid-latitudes. *Geophys. Res. Lett.* **39,** L06801 (2012).

29. Dawson, T. E., Mambelli, S., Plamboeck, A. H., Templer, P. H. & Tu, K. P. Stable Isotopes in Plant Ecology. *Annu. Rev. Ecol. Syst.* **33,** 507–559 (2002).

30. Hassanzadeh, P., Kuang, Z. & Farrell, B. F. Responses of midlatitude blocks and wave amplitude to changes in the meridional temperature gradient in an idealized dry GCM. *Geophys. Res. Lett.* **41,** 5223–5232 (2014).

31. Francis, J. A. & Vavrus, S. J. Evidence for a wavier jet stream in response to rapid Arctic warming. *Environ. Res. Lett.* **10,** 014005 (2015).

32. Kim, B.-M. *et al.* Weakening of the stratospheric polar vortex by Arctic sea-ice loss. *Nat. Commun.* **5,** 4646 (2014).

33. Alewell, C., Mitchell, M. J., Likens, G. E. & Krouse, R. Assessing the Origin of Sulfate Deposition at the Hubbard Brook Experimental Forest. *J. Environ. Qual.* **29,** 759 (2000).

34. Miles, G. R., Mitchell, M. J., Mayer, B., Likens, G. E. & Welker, J. M. Long-term analysis of Hubbard Brook stable oxygen isotope ratios of streamwater and precipitation sulfate. *Biogeochemistry* **111,** 443–454 (2012).

35. Overland, J. *et al.* The Melting Arctic and Mid-latitude Weather Patterns: Are They Connected? *J. Climate* **28**, 7917-7932 (2015).

36. Schubert, B. A. & Jahren, A. H. Seasonal temperature and precipitation recorded in the intra-annual oxygen isotope pattern of meteoric water and tree-ring cellulose. *Quat. Sci. Rev.* **125,** 1–14 (2015).

37. Klein, E. S. *et al.* McCall Glacier record of Arctic climate change: Interpreting a northern Alaska ice core with regional water isotopes. *Quat. Sci. Rev.* **131,** 274-284 (2016).

38. Campbell, J. L. *et al.* Past and projected future changes in snowpack and soil frost at the Hubbard Brook Experimental Forest, New Hampshire, USA. *Hydrol. Process.* **24,** 2465–2480 (2010).

39. Draxler, R. R. & Rolph, G. D. HYSPLIT (HYbrid Single-Particle Lagrangian Integrated Trajectory) model access via NOAA ARL READY website (http://www.arl.noaa.gov/HYSPLIT.php). NOAA Air Resources Laboratory, College Park, MD. NOAA Air Resources Laboratory (2003) (date of access: 25/09/2015).

40. Stein, A. *et al.* NOAA's HYSPLIT atmospheric transport and dispersion modeling system. *Bull. Amer. Meteor. Soc* .**96**, 2059-2077 (2015).

Acknowledgements

We would like to thank all those associated with the Hubbard Brook Ecosystem Study (HBES) who collected and archived the samples used for this research. Funding for these collections was provided by the National Science Foundation including the LTREB and LTER programs and The A. W. Mellon Foundation. This research was sponsored by the Fulbright Science and Technology Scholarship through a PhD fellowship award to T. P. Analysis for this project was conducted at the UAA Stable Isotope Laboratory supported by a NSF MRI award (0953271) to J.W. The help of Amey Bailey, Patrick McHale and Geoffrey Millard with the sample archives is most appreciated. The authors gratefully acknowledge the NOAA Air Resources Laboratory (ARL) for the provision of the HYSPLIT transport model and/or READY website (http://www.ready.noaa.gov) used in this publication. We thank to Batkhuu Dashzeveg for assistance in providing Arc GIS map.

Author Contributions

The original idea for the study came from M.M, who also contributed to the writing of the paper. T.P did most of the isotopic analyses, interpreted data including statistical analysis and generated figures, provided analyses and also contributed to the writing. J.W & E.K contributed to the writing and editing of the manuscript and to the mechanistic understanding of the isotopic findings. J.C and G.L edited several versions of the manuscript. G.L collected the precipitation samples and archived them at Hubbard Brook.

Competing Financial Interests

The authors declare no competing financial interests.

Figure Legends

Figure 1: **Long term annual mean values and trends in climate and precipitation isotopes at northeastern US site. a-e**, Results indicate a **(a)** significant increasing trend in surface air temperature (slope=0.03^{o}C yr^{-1}, P=0.0017); **(b)** no significant trend in precipitation amount (slope=2.71mm yr^{-1}, P=0.25); **(c)** significant declines in $\delta^{18}O$ (slope= -0.089‰ yr^{-1}, P<0.0001) and **(d)** $\delta^{2}H$ (slope= -0.259‰ yr^{-1}, P=0.0002); and **(e)** and a significant increase in *d-excess* (slope=0.46‰ yr^{-1}, P<0.0001).

Figure 2: **Response of HBEF precipitation $\delta^{18}O$ and *d-excess* values during the study period to AMO phase changes. a-b,** Average, de-trended AMO anomalies (^{o} C) from the Kaplan sea surface temperature V2 from http://www.esrl.noaa.gov/psd/data/timeseriesimeseries/AMO), $\delta^{18}O$=-6.78AMO-9.90, r^2=0.7 and *d-excess*=35.3AMO+12.4, r^2=0.83 **(a)** and comparison of fall precipitation $\delta^{18}O$ (blue dots) and *d-excess* value (black triangle), winter precipitation $\delta^{18}O$ (light blue dots) and *d-excess* value (red triangle) with a precipitation $\delta^{18}O$ of January-February (dark blue) and *d-excess* value (green triangle) over the 1968-2010 study period **(b)**.

Figure 3: Polar vortex event in fall of 2014. Weekly sample results are shown in graph (f) with air parcel 72-hour back trajectories (a-e). The date on x axis of the graph (f) associated with selected trajectories are presented in a-e. The maps: output of the public website service software HYSPLIT[40], https://www.ready.noaa.gov/HYSPLIT_traj.php and http://journals.ametsoc.org/doi/abs/10.1175/BAMS-D-14-00110.1

Figure 4: Air parcel back trajectories (main) and $\delta^{18}O$- *d-excess* values (inset) plot for November, 1968-2010. Five different colors indicate the 5 sources during the years associated with a negative AMO (black year numbers) and a positive AMO (white year numbers) phase. 40%, 26%, 16%, 16% 2% of trajectories show Arctic (red), Continental (green), North Atlantic (black), Mid-Atlantic (dark blue) and Pacific (purple) show, respectively. 57% of trajectories show northern sources: including Arctic and North Atlantic after the start of 1979 sea ice decline and 69% of trajectories show northern sources during positive AMO (start 1995) with higher *d-excess* values (>15‰). Figure created using ArcGIS 10.2.2.3552 (http://www.esri.com/software/arcgis/) with HYSPLIT model results[40] http://journals.ametsoc.org/doi/abs/10.1175/BAMS-D-14-00110.1.

Figure 5: **Conceptual diagram showing the direct and indirect effects of changes in ocean processes and synoptic climatology on the isotopic values of northeastern US precipitation.** Climate change is linked with decreases in Arctic sea ice and increases in the surface temperatures of the Arctic and north Atlantic oceans. These changes are linked to a reduction of the strength of the Arctic polar vortex and resultant increase in air flow in the mid-latitudes and greater frequency of incursions of Arctic air in the northeastern US. Due to changes associated with isotopic fractionation processes and the sources of precipitation, the values of $\delta^{18}O$ and $\delta^{2}H$ have declined and *d-excess* values have increased. The map of North America (https://commons.wikimedia.org/wiki/File:Cartography_of_North_America.svg) is licensed under the Attribution-Share-Alike 3.0 Unported license. The license terms can be found on the following link: https://creativecommons.org/licenses/by-sa/3.0/. Figure created using Adobe Photoshop CS6 13.01x32.

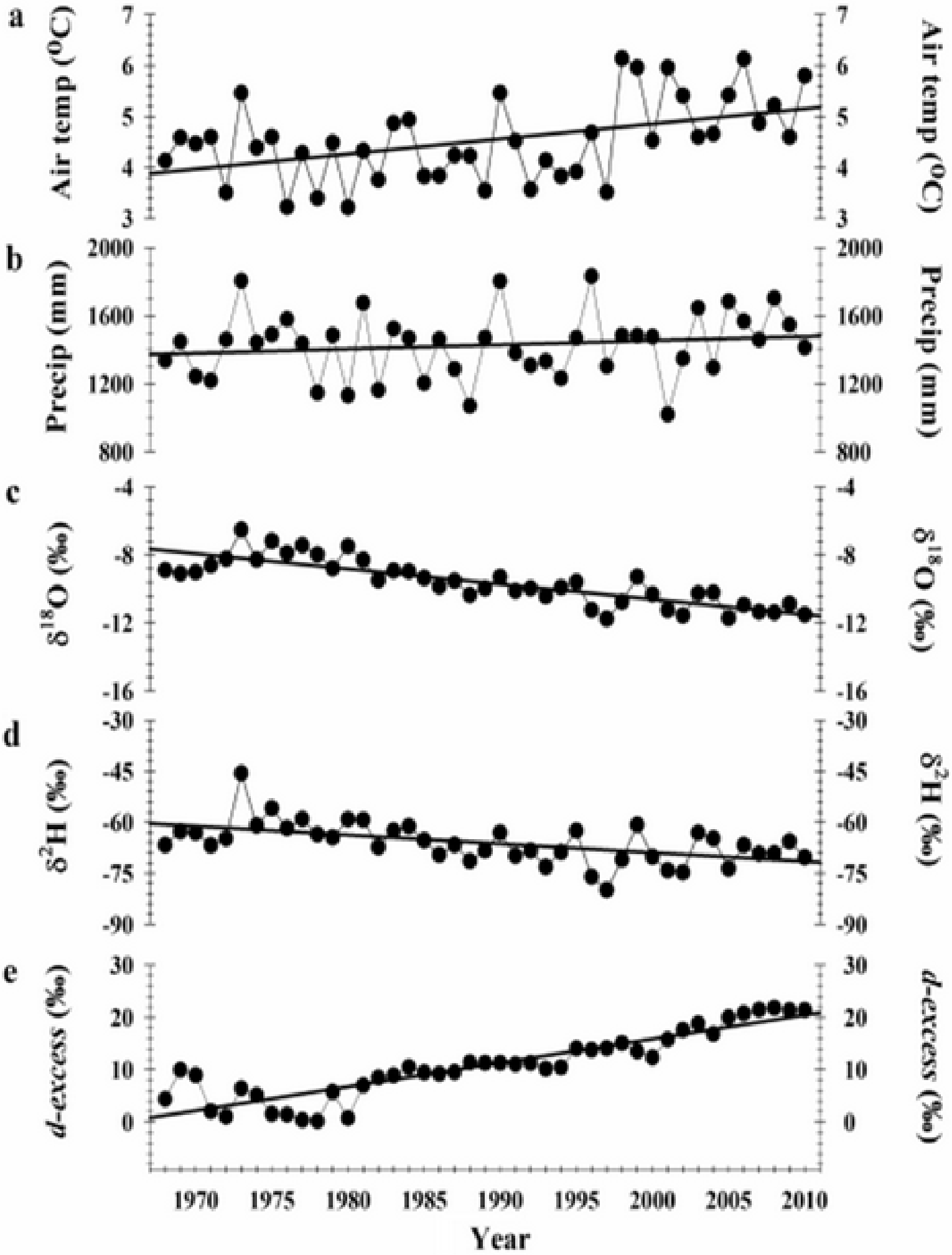
a
Air temp (°C)
7
6
5
4
3
b
Precip (mm)
2000
1600
1200
800
c
δ18O (‰)
-4
-8
-12
-16
d
δ2H (‰)
-30
-45
-60
-75
-90
e
d-excess (‰)
30
20
10
0
1970
1975
1980
1985
1990
1995
2000
2005
2010
Year

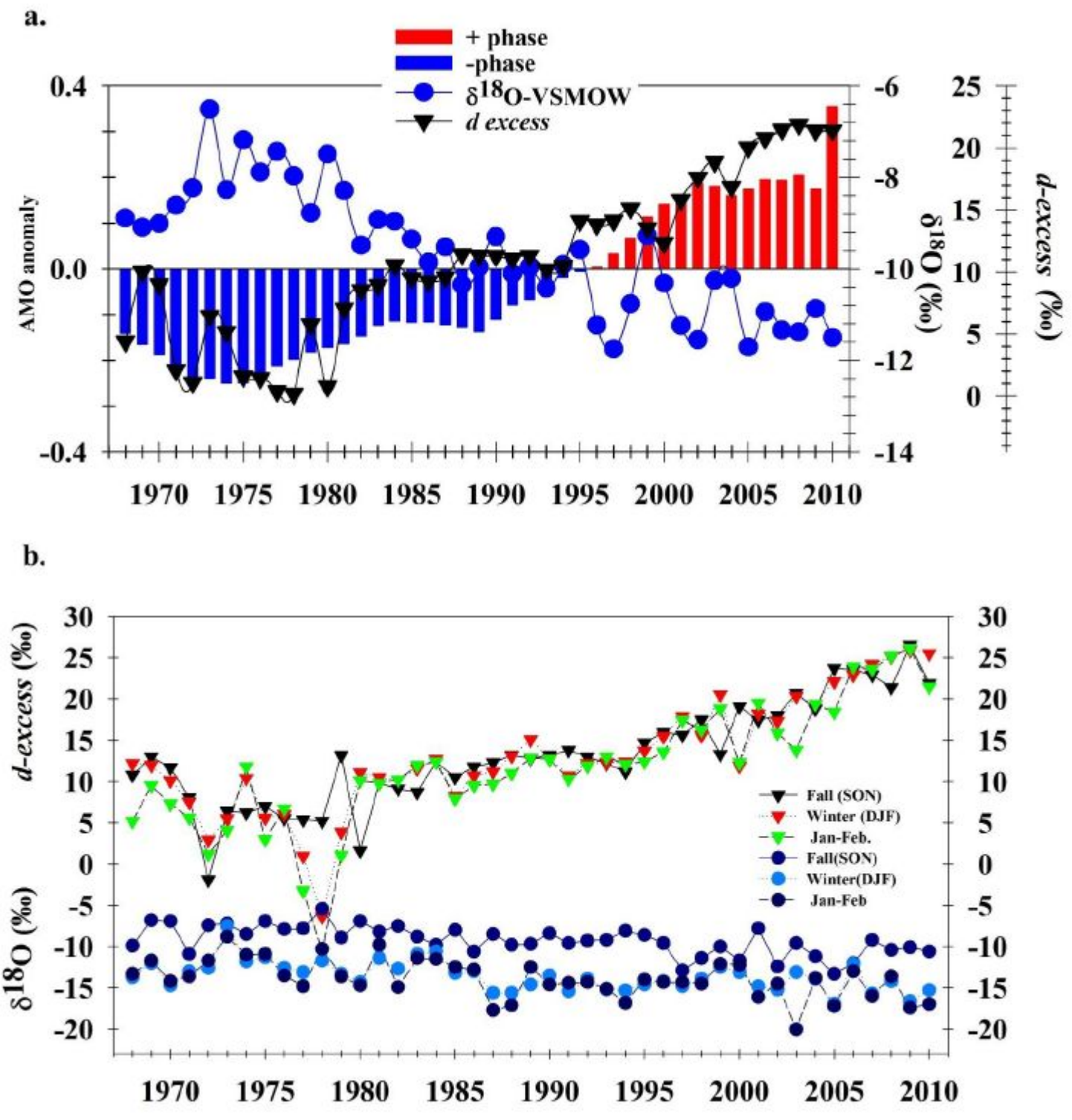
a.
+ phase
-phase
δ18O-VSMOW
d excess
AMO anomaly
δ18O (‰)
d-excess (‰)
0.4
0.0
-0.4
-6
-8
-10
-12
-14
25
20
15
10
5
0
1970
1975
1980
1985
1990
1995
2000
2005
2010
b.
d-excess (‰)
δ18O (‰)
Fall (SON)
Winter (DJF)
Jan-Feb.
Fall(SON)
Winter(DJF)
Jan-Feb
30
25
20
15
10
5
0
-5
-10
-15
-20
1970
1975
1980
1985
1990
1995
2000
2005
2010

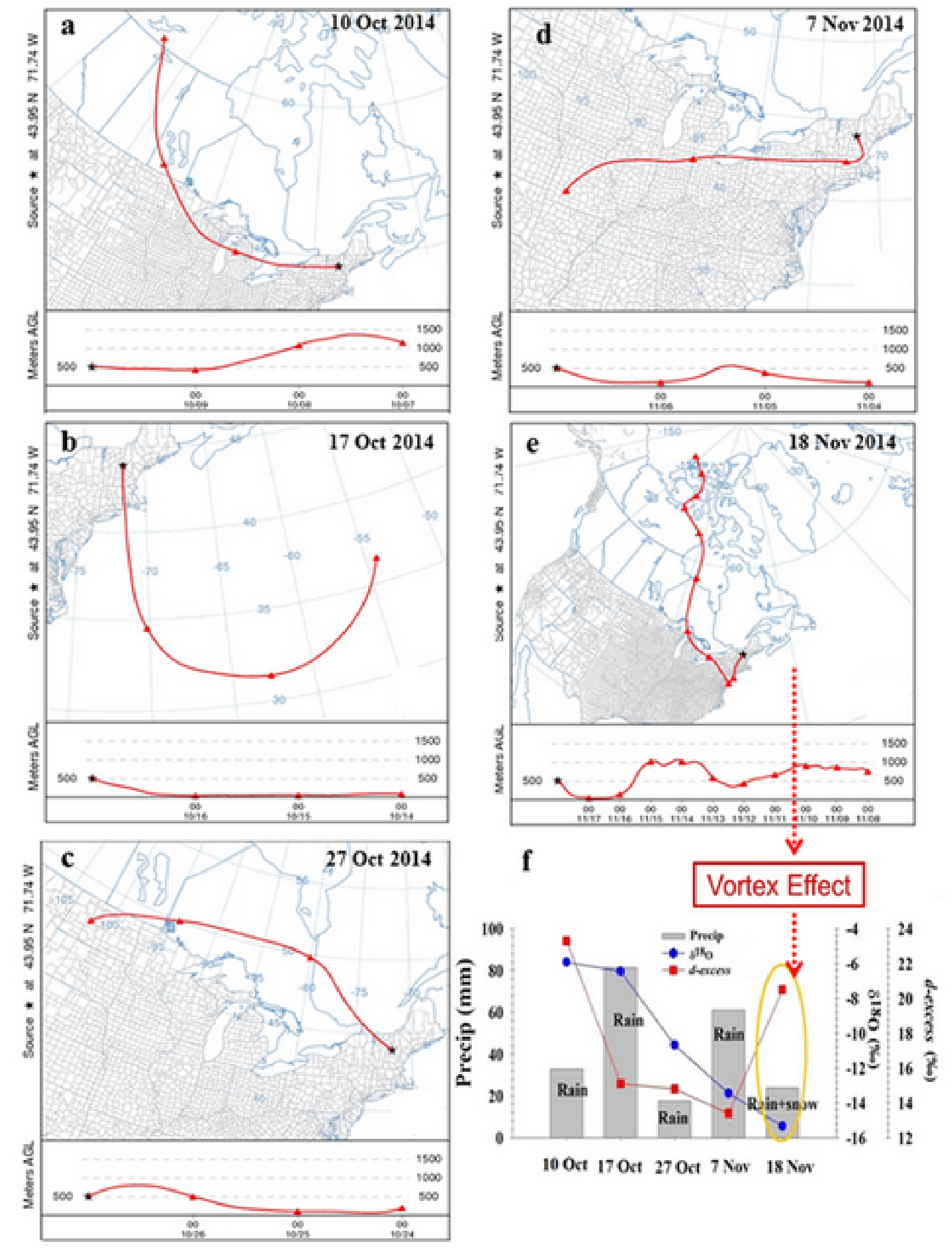
a
10 Oct 2014
b
17 Oct 2014
c
27 Oct 2014
d
7 Nov 2014
e
18 Nov 2014
Source ★ at 43.95 N 71.74 W
Meters AGL
1500
1000
500
f
Vortex Effect
Precip (mm)
Precip
δ18O
d-excess
Rain
Rain
Rain
Rain
Rain+snow
10 Oct
17 Oct
27 Oct
7 Nov
18 Nov
δ18O (‰)
d-excess (‰)

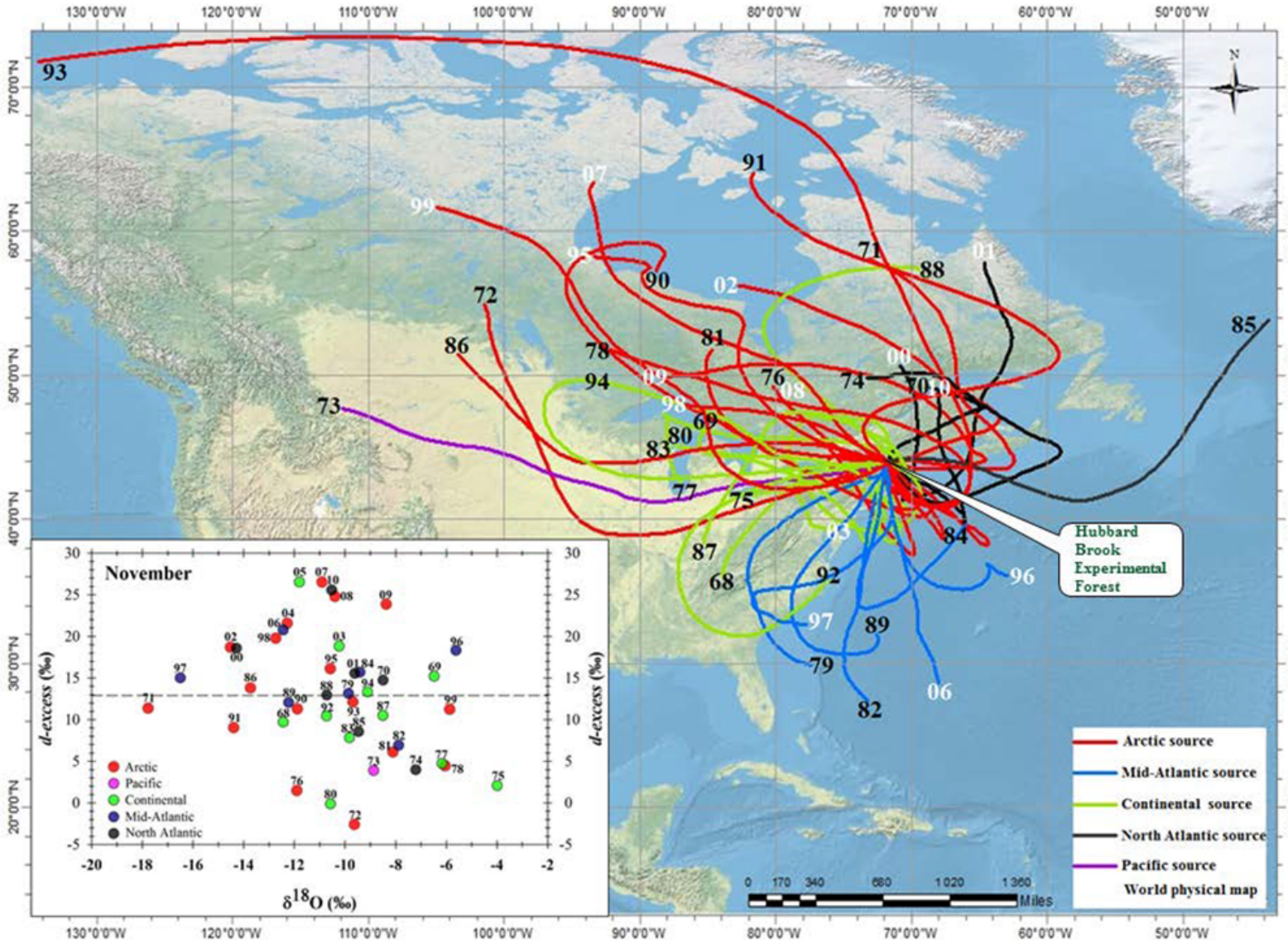
November
d-excess (‰)
δ18O (‰)
Arctic
Pacific
Continental
Mid-Atlantic
North Atlantic
Hubbard Brook Experimental Forest
Arctic source
Mid-Atlantic source
Continental source
North Atlantic source
Pacific source
World physical map
Miles

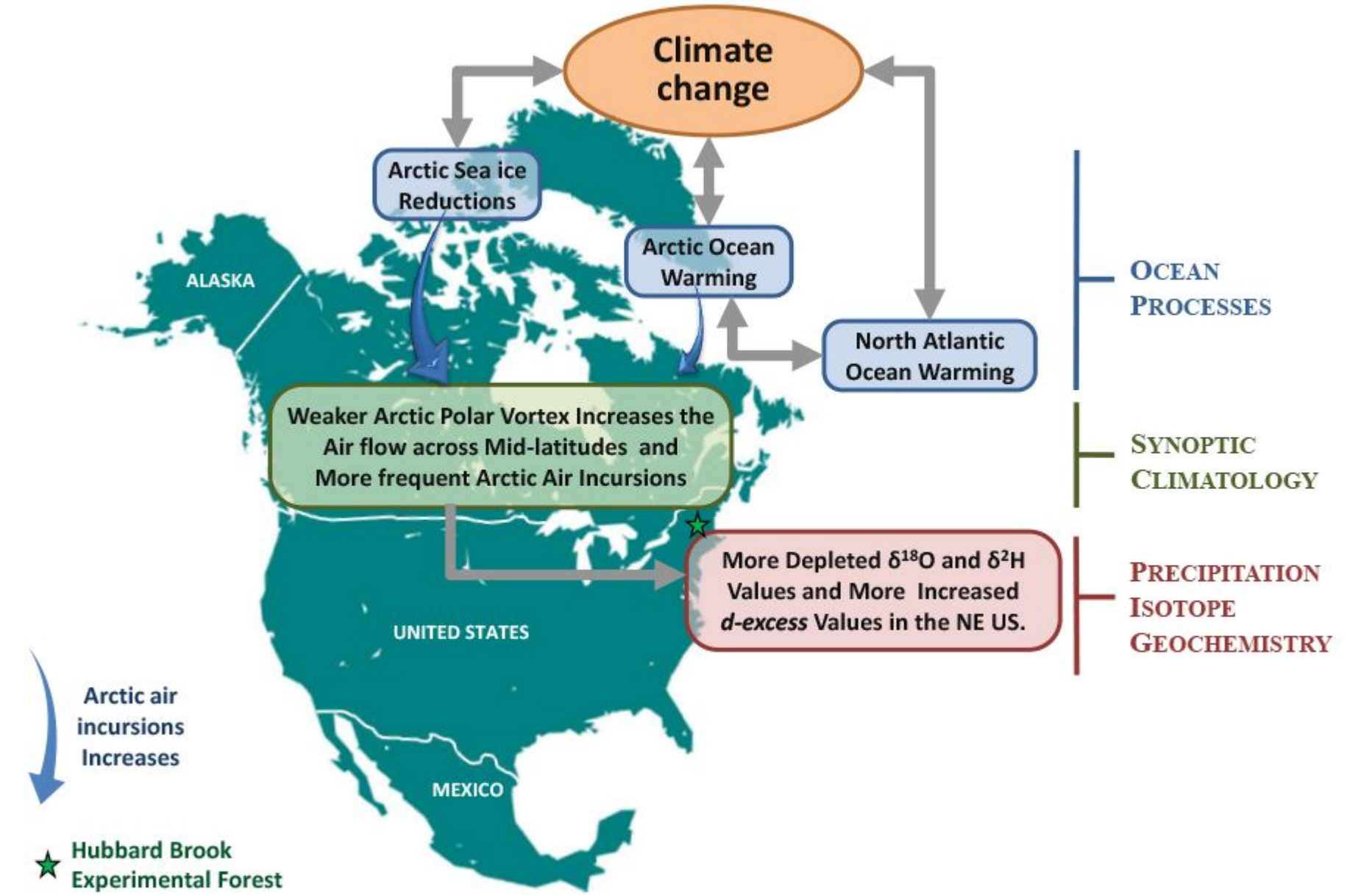
Climate change
Arctic Sea ice Reductions
Arctic Ocean Warming
North Atlantic Ocean Warming
Weaker Arctic Polar Vortex Increases the Air flow across Mid-latitudes and More frequent Arctic Air Incursions
More Depleted $\delta^{18}O$ and $\delta^{2}H$ Values and More Increased *d-excess* Values in the NE US.
ALASKA
UNITED STATES
MEXICO
Arctic air incursions Increases
Hubbard Brook Experimental Forest
OCEAN PROCESSES
SYNOPTIC CLIMATOLOGY
PRECIPITATION ISOTOPE GEOCHEMISTRY